ISSN 1674-1056
http://cpb.iphy.ac.cn
http://iopscience.iop.org/cpb
中国物理 B
Chinese Physics
中国物理 Chinese Physics B

Fractional variant of Stokes-Einstein relation in aqueous ionic solutions under external static electric fields

Gan Ren(任淦), Shikai Tian(田时开)

Citation: Chin. Phys. B . 2020, 29(3): 036101 . **doi:** 10.1088/1674-1056/ab695b
Journal homepage: http://cpb.iphy.ac.cn; http://iopscience.iop.org/cpb

What follows is a list of articles you may be interested in

Supercooled liquids analogous fractional Stokes-Einstein relation in NaCl solution above room temperature

Gan Ren(任淦), Shikai Tian(田时开)
Chin. Phys. B . 2019, 28(7): 076107 . **doi:** 10.1088/1674-1056/28/7/076107

Fractional Stokes-Einstein relation in TIP5P water at high temperatures

Gan Ren(任淦), Ge Sang(桑革)
Chin. Phys. B . 2018, 27(6): 066101 . **doi:** 10.1088/1674-1056/27/6/066101

Ab initio molecular dynamics study on the local structures in $Ce_{70}Al_{30}$ and $La_{70}Al_{30}$ metallic glasses

F X Li(李福祥), J B Kong(孔吉波), M Z Li(李茂枝)
Chin. Phys. B . 2018, 27(5): 056102 . **doi:** 10.1088/1674-1056/27/5/056102

Molecular dynamics simulations of cascade damage near the $Y_2Ti_2O_7$ nanocluster/ferrite interface in nanostructured ferritic alloys

Yi-Qiang Sun(孙祎强), Wen-Sheng Lai(赖文生)
Chin. Phys. B . 2017, 26(7): 076106 . **doi:** 10.1088/1674-1056/26/7/076106

Diffusion and thermite reaction process of film-honeycomb Al/NiO nanothermite: Molecular dynamics simulations using ReaxFF reactive force field

Hua-Dong Zeng(曾华东), Zhi-Yang Zhu(祝志阳), Ji-Dong Zhang(张吉东), Xin-Lu Cheng(程新路)
Chin. Phys. B . 2017, 26(5): 056101 . **doi:** 10.1088/1674-1056/26/5/056101

Fractional variant of Stokes–Einstein relation in aqueous ionic solutions under external static electric fields*

Gan Ren(任淦)† and Shikai Tian(田时开)

Departments of Physics & Key Laboratory of Photonic and Optical Detection in Civil Aviation, Civil Aviation Flight University of China, Guanghan 618307, *China*

(Received 3 August 2019; revised manuscript received 23 December 2019; accepted manuscript online 9 January 2020)

Both ionic solutions under an external applied static electric field E and glassy-forming liquids under undercooled state are in non-equilibrium state. In this work, molecular dynamics (MD) simulations with three aqueous alkali ion chloride (NaCl, KCl, and RbCl) ionic solutions are performed to exploit whether the glass-forming liquid analogous fractional variant of the Stokes–Einstein relation also exists in ionic solutions under E. Our results indicate that the diffusion constant decouples from the structural relaxation time under E, and a fractional variant of the Stokes–Einstein relation is observed as well as a crossover analogous to the glass-forming liquids under cooling. The fractional variant of the Stokes–Einstein relation is attributed to the E introduced deviations from Gaussian and the nonlinear effect.

Keywords: ionic solutions, Stokes–Einstein relation, non-equilibrium steady state, molecular dynamics simulation

PACS: 61.20.Ja, 78.30.cd, 82.20.Wt **DOI:** 10.1088/1674-1056/ab695b

1. Introduction

Ionic solutions play a significant role in many areas including chemical engineering[1–3] and biological systems.[4,5] The microscopic structure and transport properties of ions are two classical topics in chemical physics. The Debye–Hückel theory[6] describes ions as fully decomposed and solvated in solutions. However, recent studies suggested that ions tend to form clusters even in diluted solution.[7–10] The microscopic structures of ions are essential for many processes, including nucleation,[11,12] battery performance,[13–15] and biological systems.[16–18] Moreover, ion transport properties usually dominantly determine the performance of ionic solutions working in a non-equilibrium processes, e.g., driven by an external electric field E.

The transport properties, including diffusion and viscosity, are significantly influenced by the microscopic structure of solvation shells. Many works have been carried out to explore transport properties of ion under E. Lee and Rasaiah[19] systematically studied the extremely dilute solutions by molecular dynamics simulations. The relation between solvation structure and viscosity was also explored in extremely dilute solutions with real or virtual particles.[20] The frictional coefficients of ion were investigated under the ambient condition.[21] It was found that the charge transport and ion-ion correlation are different for different ionic solutions.[22] In addition, the concentrated NaCl solution under E was studied by several groups.[23,24] Kerisit *et al.* exploited the dynamic and transport properties of alkali ions in dimethyl sulfoxide solutions under E.[25]

The diffusion and viscosity are closely connected by the Stokes–Einstein relation $D \sim T/\eta$ in the linear response region. However, the Stokes–Einstein relation is invalid when external applied force is large, such as under a strong E.[24,25] Ionic solution is in a non-equilibrium steady state for the steady flux caused by E. The glass-forming liquids under undercooled state are also out of equilibrium for the slow dynamics. The Stokes–Einstein relation is observed to break down in glass-forming liquids and liquid metal.[13,14,26–32] Because of the difficulty to accurately determine shear viscosity η via simulation, the structural relaxation time τ is usually adopted as a substitute to evaluate the shear viscosity,[27,33–36] and the corresponding variant of the Stokes–Einstein relation is $D \sim \tau^{-1}$.[34,35] As glass-forming liquids undergo supercooling, $D \sim \tau^{-1}$ is breakdown and follows a fractional form as $D \sim \tau^{\xi}$ with $\xi \neq -1$. Since both glassy-forming liquids under undercooled state and ionic solution under strong E are out of equilibrium, but different forms of Stokes–Einstein relation are adopted in the two cases, an interesting question arises: is there an analogous fractional variant of Stokes–Einstein relation $D \sim \tau^{\xi}$ or dynamic heterogeneity existing in ionic solution under strong E?

In this work, we take three aqueous alkali chloride solutions (NaCl, KCl, and RbCl) to explore the variant of the Stokes–Einstein relation in ionic solution under strong E. The paper is organized as follows: Section 2 contains a brief description of the simulation details. The simulation results are described in Section 3. Section 4 includes our conclusions and discussion.

*Project supported by the Science Foundation of Civil Aviation Flight University of China (Grant Nos. J2019-059 and JG2019-19).

†Corresponding author. E-mail: rengan@alumni.itp.ac.cn

© 2020 Chinese Physical Society and IOP Publishing Ltd

2. Simulation details

To explore the variant of the Stokes–Einstein relation in ionic solution under E, we choose three aqueous alkali chloride (NaCl, KCl and RbCl) solutions. Each system contains 128 ion pairs and 3072 water molecules, the concentration is ~ 2.2 mol/L. Fourteen different E's uniformly distributed among 0–1.3 V/nm are applied in the X direction. The diffusion and viscosity of alkali ions have been studied by Lee *et al.*[20] In this work, we choose the same model for alkali ions and SPC/E water model. The related force field data are listed in Table 1. All our simulations are carried out with the GROMACS package,[37,38] in which the external electric field took effect on a charged atom or ion (with a partial charge q) by applying an additional electric force $F_e = qE$ in the X direction besides the routine MD forces in equilibrium, and the equation of motion for atom or ion i with mass m_i and charge q_i is

$$m_i \frac{\mathrm{d}^2 r_i}{\mathrm{d}t^2} = -\frac{\partial V\left(|r_i - r_j|\right)}{\partial r_i} + q_i E.$$

The system temperature is kept to be a constant by the Nosé–Hoover thermostat.[39,40] The periodic boundary conditions are applied in all three directions of the Cartesian space and the particle mesh Ewald algorithm[41] is employed to calculate the long-range electrostatic interactions with a cutoff of 1.2 nm in the real space. The van der Waals (VDW) interactions are calculated directly with a truncated spherical cutoff of 1.2 nm. The ion pairs including Na^+–Cl^-, K^+–Cl^-, Rb^+–Cl^- and water molecules are put in a cubic box with side lengths of 4.61 nm, 4.65 nm, 4.66 nm, respectively, which was determined by a 3-ns constant NPT MD simulation at temperature $T = 300$ K and pressure $P = 1$ atm. After a 3-ns NVT MD simulation equilibrating the system, to improve statistic, another seven 2-ns MD simulation with different initial configurations under the same condition is carried out to sample data. The time step for all the MD simulations is 1 fs and the configurations are sampled every 10 steps for further data analysis.

Table 1. The force field parameters for the Na^+, K^+, Rb^+ and SPC/E water model.

Atom/ion	σ_{io}/nm	ε_{io}/(kJ/mol)	Charge/e
Na^+	0.2876	0.5216	+1
K^+	0.325	0.5216	+1
Rb^+	0.3348	0.5216	+1
O	0.3169	0.6502	−0.8476
H	–	–	+0.4238

3. Results and discussion

Ions exists as solvated ions in aqueous ionic solution. To characterize the influence of E on solvation structure, we adopt the radial distribution function (RDF).[19] The RDF is defined as $g(r) = \langle \delta(r - r_1) \rangle$, where r_1 is the position of the central ion. The RDFs for Na^+–Cl^-, K^+-Cl^-, and Rb^+–Cl^- solution show almost the same changes under E. We only plot the RDFs for Na^+–Cl^- solution to illustrate the influence of E and the related results are shown in Fig. 1.

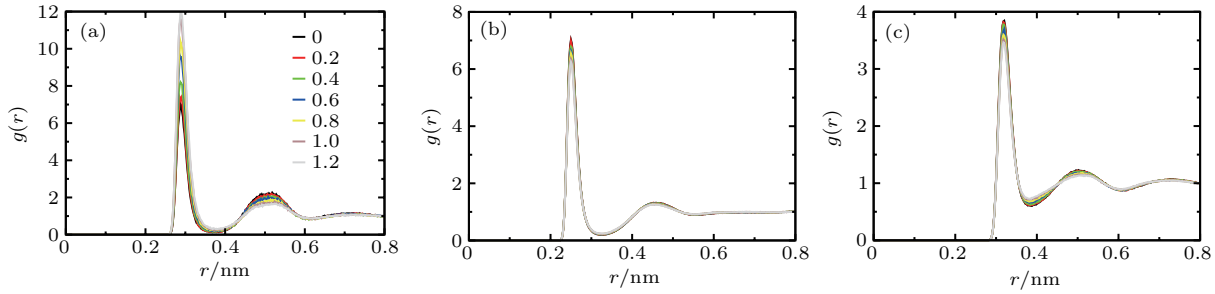


Fig. 1. Radial distribution functions (RDFs) of solvation shells under different E: (a) Na^+–Cl^- shell, (b) Na^+–H_2O shell, (c) Cl^-–H_2O shell.

Figure 1(a) shows that the main peak of the Na^+–Cl^- shell has a large increase with increasing E, whereas the second peak get a small decrease. The main peak is corresponding to the ion atmosphere, which mainly determines the dynamics of ions. The results suggest that Na^+ and Cl^- get more strong spatial correlation in the ion atmosphere. It is resulted from the decrement of dielectric constant as the dipole of water tends to get a same orientation under E.[42] The main peaks of the Na^+–H_2O shell and the Cl^-–H_2O shell have a little decrease with increasing E as shown in Figs. 1(b) and 1(c). Ion and water molecules get less spatial-correlated under a stronger E.

The variant of the Stokes–Einstein relation $D \sim \tau^{-1}$ is based on the exponential relaxation of the self-intermediate scattering function $F_s(k,t) \sim \mathrm{e}^{-t/\tau}$ in simple liquids, which can be described by $F_s(k,t) = \exp\left(-k^2 D t\right)$ if the displacements of particle follow Gaussian distribution.[28] To evaluate the variants $D \sim \tau^{-1}$, the diffusion constant of ions is calculated via the mean square displacement as

$$D = \lim_{t\to\infty} \frac{\left\langle |r_i(t) - r_i(0)|^2 \right\rangle}{6t}, \tag{1}$$

where $r_i(t)$ is the position of the i-th ion at time t, $\langle\ \rangle$ denotes the ensemble average. Ions get a unidirectional velocity under E. The displacements of ion $r(t)$ consists of two parts:[43] random diffusive displacement $r_r(t)$ due to thermal motion and unidirectional drift displacement vt. For the randomness

of $r_r(t)\lim_{t\to\infty}\langle r_r(t)\rangle = 0$, the unidirectional drift velocity can be calculated by

$$v = \lim_{t\to\infty}\langle r(t)\rangle/t. \tag{2}$$

The self-diffusion of ions is introduced by random thermal motion, so we have to deduct the unidirectional velocity in the calculation of the diffusion constant as

$$D = \lim_{t\to\infty}\frac{\langle|r_i(t) - r_i(0) - vt|^2\rangle}{6t}. \tag{3}$$

The unidirectional drift velocity v measures how far the system away from the equilibrium state.[44] The drift velocities of Na^+, K^+, Rb^+ and their corresponding Cl^- are plotted in Fig. 2. The magnitude of the velocities for each ion increases as E increases. However, because of the viscosity differences among Na^+, K^+, and Rb^+,[45] the magnitude and increasing rate of velocity for Na^+, K^+ and Rb^+ increase in an order $Na^+ < Rb^+ < K^+$. Because the electrostatic interaction decreases in the order Na^+–$Cl^- > Rb^+$–$Cl^- > K^+$–Cl^-, the magnitude and increasing rate of Cl^- increase in a reverse order. The velocities for each ion show the same changes as E increases. To quantify the variation, we redraw the velocities of Na^+ and its corresponding Cl^- in Fig. 3. The velocity increases linearly with E when $E \le 0.6$ V/nm, and follows a nonlinear relation $v \sim E + a\cdot E^2$ when $E > 0.6$ V/nm, where the quadratic term starts to play a role. The phenomenon is the Wien effect[46] that ions follow nonlinear response under strong E.

The mean square displacements (MSDs) of Na^+, K^+, Rb^+, and their corresponding Cl^- are calculated. To illustrate the MSDs under E, the results of NaCl solution is plotted in Fig. 4. The variation of MSDs for Na^+ and Cl^- with time can be separated to three regimes similar as in undercooled liquids.[28] The ballistic regime is at short times (~ 0.1 ps) so that MSD is a quadratic function in time. The diffusive regime is at long times (> 1 ps) so that MSD is a linear function in time. The cage regime is between the ballistic and the diffusive regime (0.1–1 ps), and the logarithm of MSD increases nonlinearly with logarithm of time. The MSD in the cage regime is not a plateau like undercooled liquids. The ion is not so strongly trapped in the cage as in undercooled liquids. The cage regime shortens with increasing E, and the rate of increase of MSD with time is greater under a stronger E for both Na^+ and Cl^-. This is due to fact that the unidirectional drift velocity caused ion becomes more easily to get out of the trap of solvation shell. The diffusion constants of Na^+, K^+, Rb^+ and their corresponding Cl^- calculated by Eq. (3) are plotted in Fig. 5. The diffusion constant D for each ion increases with increasing E. The tendency is almost the same for all ions and the only difference is the rate of increase.

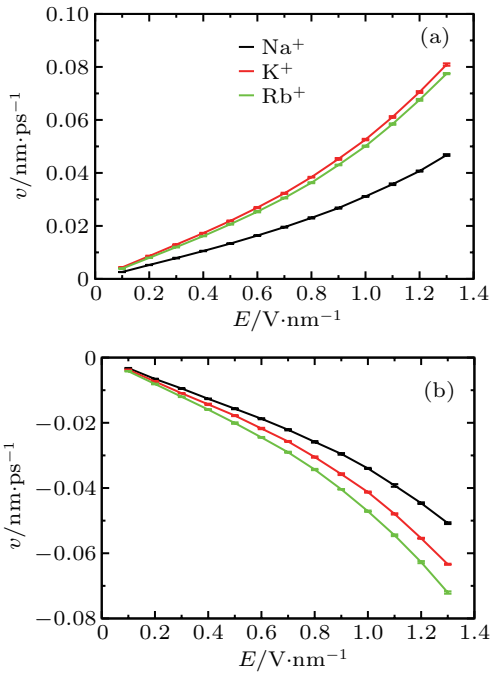


Fig. 2. The drift velocities v for Na^+, K^+, Rb^+, and their corresponding Cl^- as a function of E: (a) v for Na^+, K^+, Rb^+, (b) v for alkali ion corresponding Cl^-. The v of alkali ion corresponding Cl^- in (b) is plotted in the same color as shown in (a).

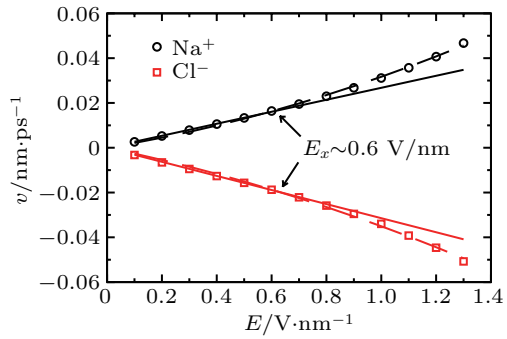


Fig. 3. The drift velocities v for Na^+ and its corresponding Cl^- versus E. The symbols are the simulated data. The solid lines are fitted by $v \sim E$ and the dotted lines are fitted by $v \sim E + a\cdot E^2$.

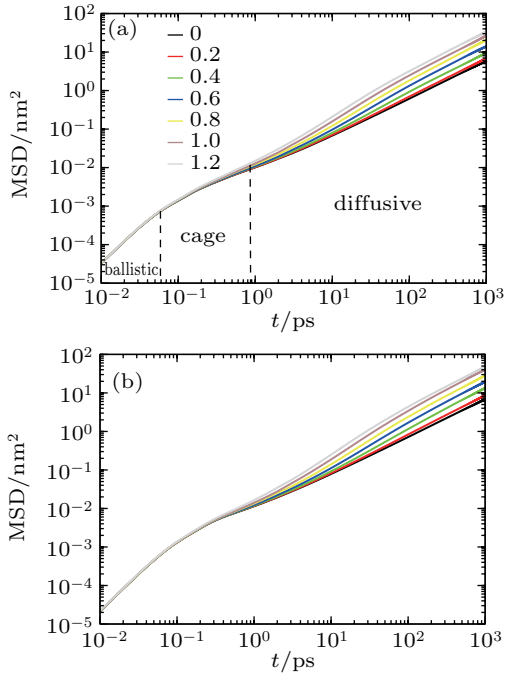


Fig. 4. The logarithm of mean square displacements for Na^+ and Cl^- as a function of the logarithm of time t under different E's: (a) Na^+, (b) Cl^-.

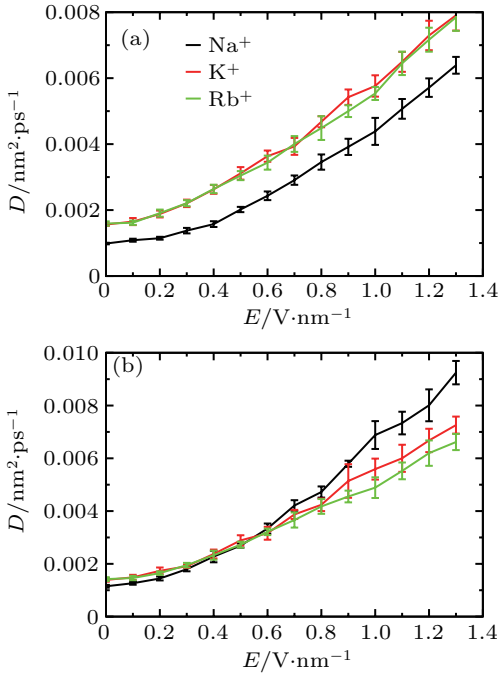


Fig. 5. The diffusion constants D of Na^+, K^+, Rb^+ and their corresponding Cl^- as a function of E. (a) D for Na^+, K^+, Rb^+, (b) D for alkali ion corresponding Cl^-. The D of alkali ion corresponding to Cl^- in (b) is plotted in the same color as shown in (a).

The structural relaxation of ion is described by the self-intermediate scattering function, namely,

$$F_s(k,t) = \frac{1}{N}\sum_j^N \left\langle \exp\left\{ i\boldsymbol{k}\cdot[r_j(0) - r_j(t)]\right\}\right\rangle, \tag{4}$$

where N is the number of ions, $r_j(t)$ is the position vector of j-th ion, k is a wavevector which is always chosen as the first maximum of the structure factor. If the ion displacement $\delta r_j(t) = r_j(t) - r_j(0)$ is Gaussian, one can express $F_s(k,t)$ in terms of the MSD as

$$F_s(k,t) = \exp\left\{-\frac{1}{2}k^2\left\langle[\delta r(t)]^2\right\rangle\right\} = \exp\left(-k^2 Dt\right), \tag{5}$$

where D is the diffusion constant. In simple liquids $F_s(k,t)$ decays exponentially like $e^{-t/\tau}$, and $D \sim \tau^{-1}$. Since the calculation of the diffusion constant has the unidirectional displacements deducted, it is also deducted in the calculation of $F_s(k,t)$. The structure factor $S(k)$ for each ion under $E = 0$ is plotted in Fig. 6. We choose wavevector k as the first maximum of $S(k)$. Here k is 21.6nm^{-1}, 16.0nm^{-1}, and 15.0 nm^{-1} for Na^+, K^+, and Rb^+, respectively, and the k values for their corresponding Cl^- are 14.0, 15.5 and 14.5 nm^{-1}. $F_s(k,t)$ for Na^+ and Cl^- in NaCl solution as an illustration is plotted in Fig. 7. It is shown that the applied E's accelerates the structural relaxation of Na^+ and Cl^-, and the ion gets a faster relaxation under a stronger E. The structural relaxation time τ for Na^+, K^+, Rb^+ and their corresponding Cl^- determined by $F_s(k,\tau) = e^{-1}$ with the chosen k is plotted in Fig. 8. The structural relaxation times for each ion all decrease with the increasing E.

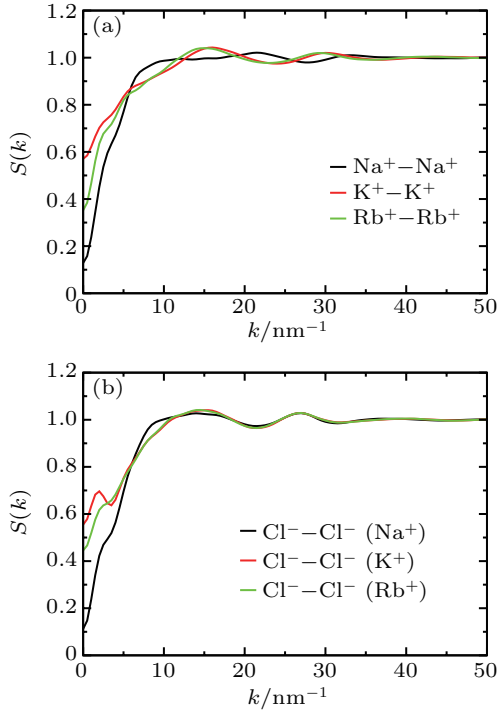


Fig. 6. The structure factor $S(k)$ for each ion under $E = 0$. $S(k)$ for Na^+, K^+, and Rb^+ are plotted in (a) and their corresponding Cl^- are plotted in (b).

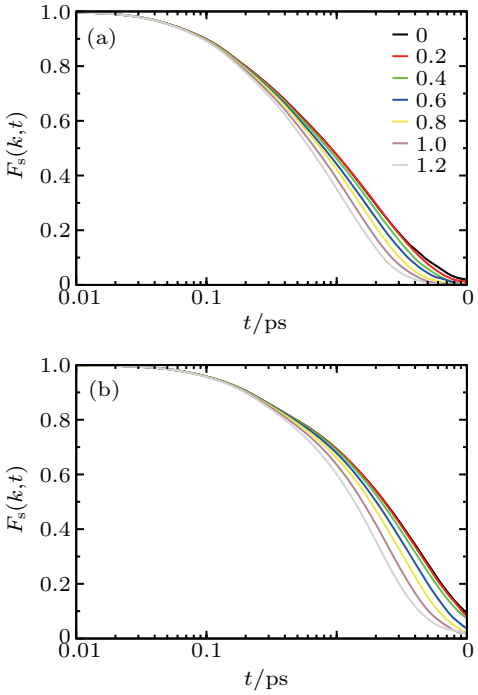


Fig. 7. The self-intermediate scattering function $F_s(k,t)$ for Na^+ and Cl^- as a function of time t under different E's: (a) Na^+, (b) Cl^-.

The simulation can be well fitted by $\log(D), \log\left(\tau^{-1}\right) \sim a + bE + cE^2$. The fitted a, b, and c are listed in Table 2. Similar to the variation of velocity with E plotted in Fig. 3, the non-linear effect also plays a role in the changes of diffusion and relation. For small E, the linear item plays a more important role E in relaxation, but the quadratic item starts to play a role with increasing E. The linear item plays a more important role than the quadratic item in diffusion for all E considered.

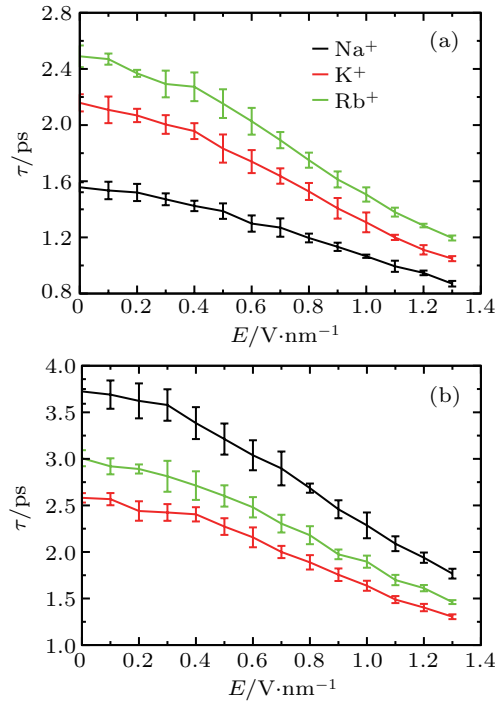


Fig. 8. The structural relaxation time τ of Na^+, K^+, Rb^+ and their corresponding Cl^- as a function of E. (a) τ for Na^+, K^+, Rb^+, (b) τ for alkali ion corresponding Cl^-. The data of alkali ion corresponding Cl^- in (b) is plotted in the same color as shown in (a).

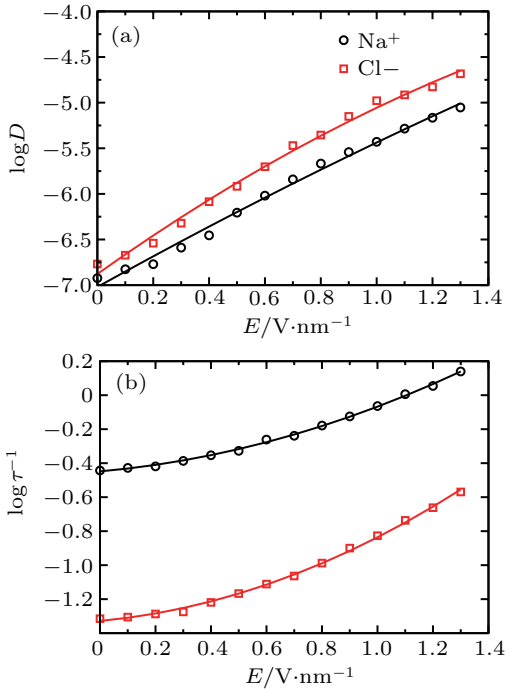


Fig. 9. The logarithms of the diffusion constant and relaxation time versus E for Na^+ and its corresponding Cl^-: (a) $\log(D)$ vs. E, (b) $\log(\tau^{-1})$ vs. E. The symbols are the simulated data and the solid lines are fitted by $\log(D), \log(\tau^{-1}) \sim a + bE + cE^2$.

Figures 5 and 8 show that the diffusion constant or relaxation times has similar changes with increasing E for all ions. To quantify the variation, the logarithms of the diffusion constant and relaxation time for Na^+, Cl^- as a function of E are plotted in Fig. 9.

To examine the existence of the fractional variant of the Stokes–Einstein relation in ionic solution under E, the variant $D \sim \tau^{-1}$ is evaluated by $D \sim \tau^{\xi}$. It will be valid if $\xi = -1$, otherwise it will follow a fractional form. The logarithms of τ^{-1} and D for Na^+, K^+, Rb^+ and their corresponding Cl^- are plotted in Fig. 10. The fitted ξ are not equal to -1 for all ions under E. The data for all ions can be well fitted by $D \sim \tau^{-\xi}$ with different ξ, and a crossover is observed for all ions with increasing E. The crossover E_x is around 0.7 V/nm, 0.5 V/nm, 0.5 V/nm for Na^+, $K^+$and Rb^+, respectively, E_x for their corresponding Cl^- is around 0.7 V/nm, 0.6 V/nm, 0.5 V/nm. The similar phenomenon is also observed in water under supercooling.[27] The exponents ξ for each ion are all different from 1 and in a fraction, which show that the fractional variant of the Stokes–Einstein relation exists in ionic solution under E.

Table 2. Fitting data of the logarithm of the diffusion constant D and structural relaxation time τ by $\log(D), \log(\tau^{-1}) \sim a + bE + cE^2$.

	D_{Na^+}	D_{Cl^-}	τ_{Na^+}	τ_{Cl^-}
a	−7.020	−6.878	−0.448	−1.328
b	1.702	2.180	0.144	0.151
c	−0.119	−0.358	0.237	0.341

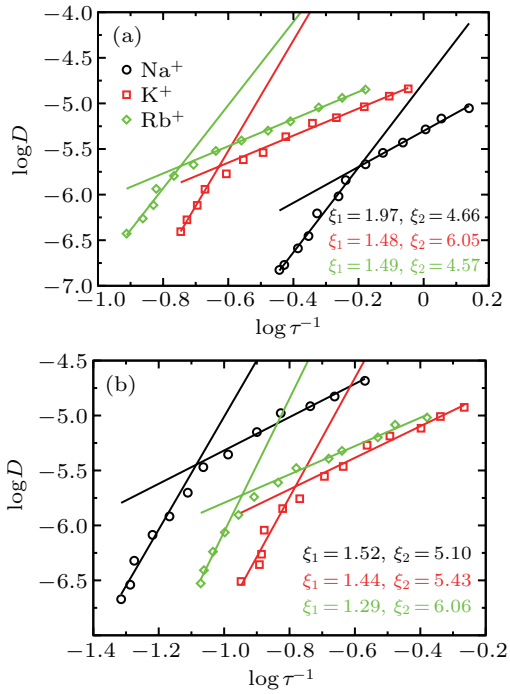


Fig. 10. Test of the variant of the Stokes–Einstein relation described by $D \sim \tau^{-1}$ for Na^+, K^+, Rb^+ and their corresponding Cl^-: (a) Na^+, $K^+$and Rb^+, (b) data for alkali ion corresponding Cl^-. The symbols are the simulated data and the solid lines are fitted by $D \sim \tau^{-\xi}$. The colored exponent ξ is corresponding to the same colored solid line. The data of alkali ion corresponding to Cl^- in (b) is plotted in the same color as shown in (a).

The variant of the Stokes–Einstein relation $D \sim \tau^{-1}$ will be a strict result if the displacements of particle follow Gaussian distribution. It is proposed that the fractional form is resulted from dynamic heterogeneity in glass-forming liquids.[47] The dynamic heterogeneity can be characterized by the deviations from Gaussian distribution in particle displacement. We calculate the self van Hove function $G_s(r,t)$ and its

first-order approximation $G_0(r,t)$ to describe the deviation.[48] $G_s(r,t)$ is the Fourier transformation of $F_s(k,t)$ and $G_0(r,t)$ takes the Gaussian form. If the distribution of ion displacement takes a Gaussian form, $G_0(r,t)$ and $G_s(r,t)$ are the same, otherwise $G_s(r,t)$ deviates from $G_0(r,t)$. The calculated results for Na^+ and Cl^- in NaCl solution at $t^* = 10$ ps are shown in Fig. 11. $G_s(r,t^*)$ deviates from the $G_0(r,t^*)$ under E. The results indicate that the dynamic heterogeneity appears under E.

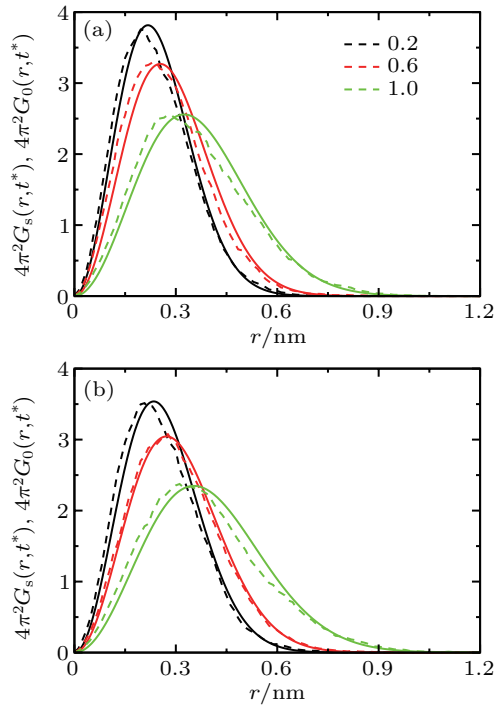


Fig. 11. Self van Hove function $G_s(r,t^*)$ and its first-order approximation $G_0(r,t^*)$ for Na^+ and Cl^- in NaCl solution at $t^* = 10$ ps under different E's. $G_s(r,t^*)$ and $G_0(r,t^*)$ are plotted in the same color with the dotted lines for $G_s(r,t^*)$ and the solid lines for $G_0(r,t^*)$.

To explore the reasons for the crossover and the fractional form observed in $D \sim \tau^{-\xi}$, as data plotted in Fig. 9 and listed in Table 2, the logarithms of the diffusion constant and structural relaxation time vary with E as $\log(D), \log(\tau^{-1}) \sim a + bE + cE^2$. The a item in diffusion is much larger than the a item in relaxation. The b item in diffusion is much greater than the c item for all E considered. Thus the response of the diffusion to E is mainly determined by the linear term in E. However, the b and c items are in the same magnitude in relaxation for all E considered. For small E, the b item is greater than the c item in relaxation but it is reverse at a large E. If we make $bE = cE^2$ in the relaxation, we can calculate the crossover E_x: $E_x = 0.607$ for Na^+, $E_x = 0.450$ for Cl^-. E_x is roughly equal to the observed linear–nonlinear crossover E_x in velocity and the crossover E_x observed in $D \sim \tau^{-\xi}$. Therefore, the fractional $D \sim \tau^{-\xi}$ and the crossover are mainly due to the linear and nonlinear effect caused by E: at small E, the linear term plays an important role and the quadratic term play a more important role at large E.

4. Conclusions

The atomistic MD simulations for aqueous NaCl, KCl and RbCl solutions have been carried out to exploit the fractional variant of the Stokes–Einstein relation in ionic solutions under strong E. Alkali ion and Cl^- get more spatially strongly correlated under a stronger E but the hydration shell is weaker. Ion gets a larger velocity with a larger E that leads the system further away from the equilibrium state. E accelerates the diffusion and structural relaxation of ion, and ion gets a greater diffusion constant and smaller relaxation time under a stronger E. The variant of the Stokes–Einstein relation is found to be breakdown under E, a fractional form and a crossover are observed as E increases. The fractional form and crossover are resulted from nonlinear response introduced by E. The fractional form and crossover are caused by the dynamic heterogeneity of ion and the linear–nonlinear response under E. Our results indicate the similarities between ionic solutions under E and glass-forming liquids, which may help us to improve our understanding and applications of ionic solutions. Moreover, the fractional variant of the Stokes–Einstein relation is caused by E in our work. Actually, some evidences have shown that both the dynamics and structures of glass-forming liquids are heterogeneous. Thus our results may make some hints on how to explain the fractional variant and crossover in glass-forming liquids under cooling, such as the heterogeneity cause molecular mean field.

Acknowledgement

The author thanks Yanting Wang (Institute of Theoretical Physics, Chinese Academy of Sciences) for suggestions.

References

[1] Equey J F, Müller S, Tsukada A and Haas O 1989 *J. Appl. Electrochem.* **19** 65
[2] Yoshida H, Sone M, Mizushima A, Abe K, Tao X T, Ichihara S and Miyata S 2002 *Chem. Lett.* **31** 1086
[3] Conway B 1992 *Chem. Soc. Rev.* **21** 253
[4] Gurau M C, Lim S M, Castellana E T, Albertorio F, Kataoka S and Cremer P S 2004 *J. Am. Chem. Soc.* **126** 10522
[5] Zhang Y and Cremer P S 2006 *Curr. Opin. Chem. Biol.* **10** 658
[6] Debye P and Hückel E 1923 *Phys. Z.* **24** 185
[7] Chialvo A, Cummings P, Cochran H, Simonson J and Mesmer R 1995 *J. Chem. Phys.* **103** 9379
[8] Bian H, Wen X, Li J, Chen H, Han S, Sun X, Song J, Zhuang W and Zheng J 2011 *Proc. Natl. Acad. Sci. USA* **108** 4737
[9] Smith D E and Dang L X 1994 *J. Chem. Phys.* **100** 3757
[10] Sherman D M and Collings M D 2002 *Geochem. Trans.* **3** 102
[11] Zahn D 2004 *Phys. Rev. Lett.* **92** 040801
[12] Ren G and Wang Y T 2015 *Chin. Phys. B* **24** 126402
[13] Swallen S F, Bonvallet P A, McMahon R J and Ediger M D 2003 *Phys. Rev. Lett.* **90** 015901
[14] Mapes M K, Swallen S F and Ediger M D 2006 *J. Phys. Chem. B* **110** 507
[15] White J A 1999 *J. Chem. Phys.* **111** 9352
[16] Barrat J L, Roux J N and Hansen J P 1990 *Chem. Phys.* **149** 197
[17] Thirumalai D and Mountain R D 1993 *Phys. Rev. E* **47** 479
[18] Yi S S, Pan C and Hu Z H 2015 *Chin. Phys. B* **24** 120201

[19] Lee S H and Rasaiah J C 1994 *J. Chem. Phys.* **101** 6964
[20] Koneshan S, Rasaiah J C, Lynden-Bell R and Lee S 1998 *J. Phys. Chem. B* **102** 4193
[21] Koneshan S, Lynden-Bell R and Rasaiah J C 1998 *J. Am. Chem. Soc.* **120** 12041
[22] Kashyap H K, Annapureddy H V, Raineri F O and Margulis C J 2011 *J. Phys. Chem. B* **115** 13212
[23] Ren G, Shi R and Wang Y 2014 *J. Phys. Chem. B* **118** 4404
[24] Murad S 2011 *J. Chem. Phys.* **134** 114504
[25] Lewis L J and Wahnström G 1994 *Phys. Rev. E* **50** 3865
[26] Mallamace F, Broccio M, Corsaro C, Faraone A, Wanderlingh U, Liu L, Mou C Y and Chen S H 2006 *J. Chem. Phys.* **124** 161102
[27] Xu L, Mallamace F, Yan Z, Starr F W, Buldyrev S V and Eugene Stanley H 2009 *Nat. Phys.* **5** 565
[28] Binder K and Kob W 2011 *Glassy materials and disordered solids: An introduction to their statistical mechanics* (Singapore: World Scientific)
[29] Habasaki J, Leon C and Ngai K 2017 *Top. Appl. Phys.* **132**
[30] Zhou Y H, Han X J and Li J G 2019 *J. Non-Cryst. Solids* **517** 83
[31] Han X J and Schober H R 2011 *Phys. Rev. B* **83** 224201
[32] Li C H, Han X J, Luan Y W and Li J G 2017 *Chin. Phys. B* **26** 016102
[33] Kumar P, Buldyrev S V, Becker S R, Poole P H, Starr F W and Stanley H E 2007 *Proc. Natl. Acad. Sci. USA* **104** 9575
[34] Jeong D, Choi M Y, Kim H J and Jung Y 2010 *Phys. Chem. Chem. Phys.* **12** 2001
[35] Ikeda A and Miyazaki K 2011 *Phys. Rev. Lett.* **106** 015701
[36] Ren G and Sang G 2018 *Chin. Phys. B* **27** 066101
[37] Berendsen H J, van der Spoel D and van Drunen R 1995 *Comput. Phys. Commun.* **91** 43
[38] Van Der Spoel D, Lindahl E, Hess B, Groenhof G, Mark A E and Berendsen H J 2005 *J. Comput. Chem.* **26** 1701
[39] Nosé S 1984 *J. Chem. Phys.* **81** 511
[40] Hoover W G 1985 *Phys. Rev. A* **31** 1695
[41] Essmann U, Perera L, Berkowitz M L, Darden T, Lee H and Pedersen L G 1995 *J. Chem. Phys.* **103** 8577
[42] Anderson J, Ullo J J and Yip S 1987 *J. Chem. Phys.* **87** 1726
[43] Shi R and Wang Y 2013 *J. Phys. Chem. B* **117** 5102
[44] Wolynes P G and Lubchenko V 2012 *Structural glasses, supercooled liquids: Theory, experiment and applications* (New York: John Wiley & Sons)
[45] Lee S H and Rasaiah J C 1996 *J. Phys. Chem.* **100** 1420
[46] Onsager L and Kim S K 1957 *J. Phys. Chem.* **61** 198
[47] Berthier L and Biroli G 2011 *Rev. Mod. Phys.* **83** 587
[48] Kob W, Donati C, Plimpton S J, Poole P H and Glotzer S C 1997 *Phys. Rev. Lett.* **79** 2827